


RESEARCH ARTICLE

Brain PET substrate of impulse control disorders in Parkinson's disease: A metabolic connectivity study

Antoine Verger^{1,2,3} | Elsa Klesse^{4,5} | Mohammad B. Chawki² | Tatiana Witjas^{4,5} |
Jean-Philippe Azulay^{4,5} | Alexandre Eusebio^{4,5*} | Eric Guedj^{1,5,6*} 

¹Department of Nuclear Medicine, Assistance Publique-Hôpitaux de Marseille, Aix-Marseille Université, Timone University Hospital, Provence-Alpes-Côte d'Azur, France

²Department of Nuclear Medicine & Nancyclotep Imaging platform, CHRU Nancy, Nancy F-54000, France

³Université de Lorraine, INSERM, IADI, Nancy F-54000, France

⁴Department of Neurology and Movement Disorders, Assistance Publique-Hôpitaux de Marseille, Aix-Marseille Université, Timone University Hospital, Provence-Alpes-Côte d'Azur, France

⁵Aix Marseille Univ, CNRS, Centrale Marseille, Institut Fresnel, Marseille, France

⁶CERIMED, Aix-Marseille Université, Marseille, France

Correspondence

Eric Guedj, MD, PhD, Service Central de Biophysique et Médecine Nucléaire, Hôpital de la Timone, 264 rue Saint Pierre, 13005 Marseille, France.
Email: eric.guedj@ap-hm.fr

Funding information

"Investissements d'Avenir" French Government program, Grant/Award Number: ANR-11-IDEX-0001-02; Inserm (Centre d'Investigation Clinique, CIC, Hôpital de la Conception, Marseille); AP-HM, Grant/Award Number: PHRC 2007/09

Abstract

Impulse control disorders (ICDs) have received increased attention in Parkinson's disease (PD) because of potentially dramatic consequences. Their physiopathology, however, remains incompletely understood. An overstimulation of the mesocorticolimbic system has been reported, while a larger network has recently been suggested. The aim of this study is to specifically describe the metabolic PET substrate and related connectivity changes in PD patients with ICDs. Eighteen PD patients with ICDs and 18 PD patients without ICDs were evaluated using cerebral 18F-fluorodeoxyglucose positron emission tomography. SPM-T maps comparisons were performed between groups and metabolic connectivity was evaluated by interregional correlation analysis (IRCA; $p < .005$, uncorrected; $k > 130$) and by graph theory ($p < .05$). PD patients with ICDs had relative increased metabolism in the right middle and inferior temporal gyri compared to those without ICDs. The connectivity of this area was increased mostly with the mesocorticolimbic system, positively with the orbitofrontal region, and negatively with both the right parahippocampus and the left caudate (IRCA). Moreover, the betweenness centrality of this area with the mesocorticolimbic system was lost in patients with ICDs (graph analysis). ICDs are associated in PD with the dysfunction of a network exceeding the mesocorticolimbic system, and especially the caudate, the parahippocampus, and the orbitofrontal cortex, remotely including the right middle and inferior temporal gyri. This latest area loses its central place with the mesocorticolimbic system through a connectivity dysregulation.

KEYWORDS

FDG-PET, impulse control disorders, metabolic connectivity, Parkinson's disease

1 | INTRODUCTION

Impulse control disorders (ICDs) have received increased attention in Parkinson's disease (PD) because of potentially dramatic consequences (Witjas, Eusebio, Fluchère, & Azulay, 2012). ICDs may affect up to one-third of patients, with various rates depending on the type (i.e., compulsive eating, pathological gambling, compulsive shopping, and hypersexuality) (Maréchal et al., 2015). The management of ICDs is often

difficult, particularly in case of advanced PD, leading to a reduction of dopaminergic treatment at the expense of motor symptoms (Zhang et al., 2016). Although some risk factors have been identified (i.e., male gender, younger age, early onset PD, personal or familial history of ICDs, substance abuse or novelty seeking, and risk taking behaviours) (Weintraub et al., 2010), the exact mechanisms underlying ICDs remain incompletely understood.

In the absence of PD, ICD patients with pathological gambling showed striatal hyperactivations during a functional magnetic resonance imaging (fMRI) gambling task (Frosini et al., 2010). The striatum is part of

*Alexandre Eusebio and Eric Guedj are the co-last authors.

the mesocorticolimbic system, which also includes the ventral tegmental area, prefrontal cortex, amygdala, and hippocampus. This network is well-known to be involved in reward processing (Koob & Volkow, 2010) and addictions (D'Ardenne, McClure, Nystrom, & Cohen, 2008). The involvement of structures of the mesocorticolimbic system has also been confirmed using resting-state single photon emission tomography (SPECT) perfusion in PD patients with pathological gambling (Cilia et al., 2008). On the other hand, in a more consistent population of PD patients with pathological gambling, Cilia et al. (2011) showed later a positive correlation between gambling score and SPECT perfusion of the left fusiform gyrus and the cerebellum, suggesting a complementary network.

Connectivity analyses are useful to better understand networks involved in brain pathologies (Fox & Greicius, 2010). To the best of our knowledge, only three studies have investigated resting-state connectivity in patients with PD and ICDs (Carriere, Lopes, Defebvre, Delmaire, & Dujardin, 2015; Cilia et al., 2011; Tessitore et al., 2017). Using perfusion SPECT, Cilia et al. showed connectivity changes between the anterior cingulate and striatum in PD patients with pathologic gambling (Cilia et al., 2011). Using fMRI, Carriere et al. (2015) found more diffuse cortico-striatal changes in PD patients with various ICDs, suggesting the involvement of a larger network, not strictly limited to the mesocorticolimbic system. In another study using fMRI, Tessitore et al. (2017) found an increased connectivity within the salience and default-mode networks, as well as a decreased connectivity within the central executive network in PD patients with ICDs.

If ^{18}F -fluoro-deoxy-glucose (^{18}F -FDG) positron emission tomography (PET) has been widely used to explore movement disorders including PD (Gesquière-Dando et al., 2015), it was never used so far to explore the metabolic substrate of ICDs in patients with PD. This functional resting-state imaging technique evaluates cerebral metabolic rate of glucose (CMRGlC), and has been recently extended to the study of metabolic connectivity using inter-regional correlation analysis (IRCA) (Lee et al., 2008), with a better spatial resolution than SPECT (Bailey & Willowson, 2014). Recently, metabolic connectivity has also been explored using graph theory analysis, allowing connectivity study in overall cerebral areas or in subgroups of clusters (Mijalkov et al., 2017). Compared to fMRI, technical performances of PET instrumentation are of course less favorable, but with an original targeting of the glucose consumption that is known to precede the transient relative decrease of BOLD signal (Magistretti & Pellerin, 1999), without any magnetic limitations, and rather better signal-to-noise ratios, variance concentration, and out-of-sample replication at single-level than fMRI. The competitive advantages of this emerging approach have been described recently (Yakushev, Drzezga, & Habek, 2017).

The aim of this study was to specifically describe the metabolic PET substrate and related connectivity changes in PD patients with ICDs, in comparison to PD patients without ICDs and to healthy controls.

2 | MATERIALS AND METHODS

2.1 | Study population and clinical evaluation

Diagnostic criteria of PD used in this study are those of the UK Parkinson's Disease Society Brain Bank criteria (Defer, Widner, Marié, Rémy, &

Levivier, 1999). Among PD patients referred to our center from 2008 to 2013 with at least five years of disease duration, 18 patients were identified as having ICDs. This threshold was selected because disease duration is considered as a risk factor of ICDs onset (Nombela, Rittman, Robbins, & Rowe, 2014). We excluded patients with: cognitive decline ($\leq 123/144$ on Mattis score; Llebaria et al., 2008), major depressive state, or a history of ICDs before disease onset. The eighteen PD patients with ICDs were matched with eighteen PD patients without ICDs, excluding non-ICD patients with criteria for Dopaminergic Dysregulation Syndrome (DDS) (Giovannoni, O'Sullivan, Turner, Manson, & Lees, 2000). These two groups were similar for age, gender, disease duration, AFPA scale (French assessment of socio-professional level), LEDD (Levodopa Equivalent Daily Dose), UPDRS-III (Unified Parkinson's Disease Rating Scale) score in OFF, Hoehn, and Yahr stage in OFF and Mattis scale, as detailed in Table 1. In addition to the interview, behavioral disorders were prospectively assessed using the Minnesota impulse disorder inventory (MIDI) and the Diagnostic and Statistical Manual of Mental Disorders, 4th Edition, Text Revision (DSM-IV-TR) criteria for substance misuse, binge eating, and pathological gambling. Giovannoni's criteria were used for Dopamine Dysregulation Syndrome (Giovannoni et al., 2000). The Questionnaire for Impulsive-Compulsive Disorders in Parkinson's Disease-Rating Scale (QUIP-RS) was not used at the time of this study. Therefore, only qualitative assessments of ICDs could be performed. However, the existence of multiple ICDs was taken as a measure of severity (see results). Apathy and mood evaluations were also performed with Lille Apathy Rating Scale (LARS) and Beck Depression Inventory (BDI).

Levodopa Equivalent Daily Dose (LEDD) and the equivalent for dopamine agonists (DA-LEDD) were calculated for patients with PD, according to guidelines (Tomlinson et al., 2010). Laterality of the PD was calculated using the motor asymmetry index (Holtgraves, McNamara, Cappaert, & Durso, 2010).

Finally, a group of 18 healthy subjects was extracted from a local normal ^{18}F -FDG PET database constituting a control population (Clinical Trials Ref: NCT00484523) approved by our local ethics committee, with similar age, gender, and level of education than those of patients' groups ($p > .39$; 61.3 ± 7.9 years, 6 women, AFPA socio-professional score: 3.7 ± 1.3). All patients and controls participated with written informed consent in agreement with the Declaration of Helsinki.

2.2 | ^{18}F -FDG PET acquisition and analysis

^{18}F -FDG PET were performed under the same conditions for all patients and healthy subjects, using an integrated PET/scanner (CT) camera (Discovery ST, GE Healthcare, Waukesha, WI) with an axial resolution of 6.2 mm allowing 47 contiguous transverse sections of the brain of 3.27 mm thickness. ^{18}F -Fluorodesoxyglucose (^{18}F -FDG) (150 MBq) was injected intravenously with the subject in an awake and resting state with eyes closed in a quiet environment. Image acquisition was started 30 min after injection and was ended 15 min later. Images were reconstructed using the ordered subsets expectation maximization algorithm with 5 iterations and 32 subsets, and corrected for attenuation using a CT transmission scan.

Whole-brain statistical analysis was performed at voxel-level using SPM8 software (Wellcome Department of Cognitive Neurology,

TABLE 1 Patient characteristics

	ICD (n = 18)	Without ICD (n = 18)	p value
Age (years)	60.4 ± 7.3	61.8 ± 6.4	.53
Gender (male)	15 (83%)	10 (56%)	.07
Duration of Parkinson's disease (years)	10.9 ± 3.6	12.2 ± 2.9	.23
LEDD-DA (mg)	157.3 ± 130.0	205.4 ± 162.8	.33
Total LEDD (mg)	1124.1 ± 320.5	1145.9 ± 378.4	.85
UPDRS-III (off) (/108)	31.9 ± 12.0	30.8 ± 12.0	.77
UPDRS-III (on) (/108)	5.3 ± 4.1	8.8 ± 6.2	.06
Hoehn and Yahr (off) (/5)	2.7 ± 0.8	2.7 ± 0.8	.88
Mattis (/144)	138.2 ± 6.2	137.8 ± 5.9	.87
BDI (63)	11.3 ± 7.4	8.4 ± 4.7	.22
LARS (from -36 to 36)	-24.5 ± 16.4	-32.9 ± 4.2	.34
AFPA (/5)	3.3 ± 1.4	3.4 ± 1.4	.72
Motor laterality index of the disease	7/3/8	5/4/9	.77
(Right/left/bilateral)	4 (22%)	3 (17%)	.67
Current smoking			

Note. Abbreviations: AFPA = Assessment of Professional Level; BDI = Beck Depression Inventory; LARS = Lille Apathy Rating Scale; LEDD = L-Dopa Equivalent Daily Dose; UPDRS = Unified Parkinson's Disease Rating Scale.

University College, London, UK) to compare ICD, non-ICD patients, and healthy controls by using ANOVA (Analysis of Variance) tests. The PET images were spatially normalized onto the Montreal Neurological Institute (MNI) atlas. The dimensions of the resulting voxels were $2 \times 2 \times 2$ mm. The images were then smoothed with a Gaussian filter (8 mm full-width at half-maximum) to blur individual variations in gyral anatomy and to increase the signal-to-noise ratio. The between-groups SPM (T) maps were obtained at a threshold (voxel-level significance) of $p < .005$, uncorrected at voxel-level, but with a correction for cluster volume to avoid type II errors ($k > 130$), as recommended (Lieberman & Cunningham, 2009), with age, gender, and level of education as nuisance covariates. An additional analysis with small volume correction (SVC) was applied within the most significant voxel of the previous identified cluster. The Proportional scaling was applied, giving the same global value to each PET examination, to correct for individual variations in global brain metabolism. The anatomical localization of the most significant voxels was then identified using Talairach Daemon (<http://ric.uthscsa.edu/projects/talairachdaemon.html>). The mean values of cerebral metabolic rate of glucose (CMRGlc) were extracted at the individual level for each significant cluster.

To evaluate metabolic connectivity, two different approaches have been performed. First, interregional correlation analysis (IRCA) was carried out according to the procedure validated by Lee et al. (2008), using the metabolic cluster previously identified in the intergroup comparison as a covariate. Briefly, mean values of CMRGlc were used as interacted covariates to find regions showing significant voxel-wise negative/positive correlations across patients with ICDs, patients without ICDs and healthy controls groups (intragroup analysis), and afterward for the

direct comparison between patients with and without ICDs (between-group analysis). Results were expressed as an increase of positive or negative connectivity as previously reported (Kaiser, Andrews-Hanna, Wager, & Pizzagalli, 2015). Nuisance covariates and threshold were the same as previously detailed for groups SPM (T) maps comparisons.

Second, a graph theory analysis was carried out with BRAPH (BRain Analysis using graph theory (<http://www.brapph.org/>), a software package to perform graph theory analysis of the brain connectome, to compare the brain's connectivity in patients with and without ICDs, and in healthy subjects, and especially relationships between clusters previously identified in the intergroup comparison and meso-corticolimbic system (Mijalkov et al., 2017; Pereira et al., 2015). Spearman correlation coefficients were computed and absolute values kept. Nodal measures and comparisons were performed using weighted undirected graphs. Tested nodal parameters were degree, strength, triangles, eccentricity, path length, global and local efficiency, clustering nodes, betweenness and closeness centrality, and within module z-score degree. Nonparametric permutation tests with 1,000 permutations were carried out to assess differences between groups.

2.3 | Statistical analysis of clinical and demographic characteristics

Quantitative variables are expressed as means ± standard deviations, and categorical variables as percentages. Statistical parameters for SPM analysis and graph theory are detailed above. *T* tests were done for mean comparisons for quantitative variables while Chi-2 Test were done for categorical variables. The significance level *p* value was set at .05.

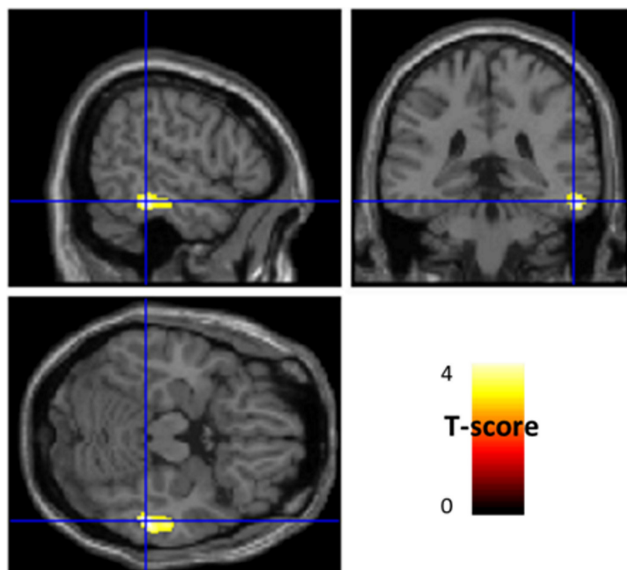


FIGURE 1 Anatomical localization of areas of increased metabolism in ICD patients in comparison to without ICDs ($p < .005$, uncorrected, $k > 130$) projected onto sections of a normal MRI set spatially normalized and smoothed into the standard SPM8 template. In comparison to patients without ICDs, those with ICDs showed a relative increased metabolism in right middle and inferior temporal gyri (BA20–21). ICD: impulse control disorders; MRI: magnetic resonance imaging; BA: Brodmann area [Color figure can be viewed at wileyonlinelibrary.com]

3 | RESULTS

3.1 | Patient characteristics

Characteristics of patients with and without ICDs are detailed in Table 1. Among patients with ICDs, 9 had a single ICD (4 “pathological

gambling,” 3 “compulsive shopping,” and 2 “hypersexuality”), and 9 had two concomitant ICDs (4 “hypersexuality and pathological gambling,” 3 “compulsive shopping and pathological gambling,” and 2 “hypersexuality and compulsive buying”). Otherwise, 3 patients with ICDs had associated dopamine dysregulation syndrome.

As reported in Table 1, there was no significant difference between patients with and without ICDs in BDI and in LARS. Furthermore, there was also no significant difference for motor asymmetry index in PD between the two categories of patients. Finally, no difference in Mattis score was found between patients with PD and healthy controls.

3.2 | ¹⁸F-FDG PET findings

In comparison to patients without ICDs, those with ICDs had a relative increased metabolism in right middle and inferior temporal gyri (Brodmann areas (BA) 20–21) ($p < .005$, uncorrected, $k > 130$; Figure 1 and Table 2). An additional analysis with SVC (previous identified cluster of 1,736 mm³ with center coordinates at 58.1; –30.3; –18.2, i.e., the most significant voxel of the right middle/inferior temporal cluster), secondarily identified a significant cluster of decreased metabolism for comparisons between patients with ICDs and healthy controls and between those without ICDs and healthy controls (after SVC for this same voxel threshold, $p_{\text{cluster}} = .05$ and $.02$ respectively, FWE-corrected).

In addition, mean CMRGlc values of right BA20–21 were higher in patients with multiple ICDs in comparison to those with single ICDs ($p = .03$).

No decrease of metabolism was observed in patients with ICDs in comparison to those without ICDs.

We thereafter studied the metabolic connectivity of this right middle/inferior temporal cluster using IRCA, within (Figure 2) and between (Figure 3) subjects’ groups ($p < .005$, uncorrected, $k > 130$). Patients with ICDs showed a diffuse positive connectivity in bilateral posterior

TABLE 2 ¹⁸F-FDG-PET findings between ICD and non-ICD patients (anatomical locations, spatial extents of significant clusters, Talairach coordinates, maximal z-scores, and height threshold of peak-voxel)

	Cluster dimension	Peak coordinates			z-score of Peak	p value
		x	y	z		
Relative hypermetabolism in ICD patients, in comparison to those without ICDs						
Right middle and inferior temporal gyri (BA20–21)	217	56	–36	–18	3.52	<.001
Increased positive connectivity with BA20–21R in ICD patients in comparison to those without ICDs						
Right middle temporal gyrus (BA20–21-22)	1425	46	10	46	3.68	<.001
Right middle and inferior frontal gyri (BA9–10-11)	177	62	–36	–20	3.62	<.001
Right middle and superior temporal gyri and parietal inferior lobule (BA37–39-40)	898	58	–58	26	3.60	<.001
Increased negative connectivity with BA20–21R in ICD patients in comparison to those without ICDs						
Left Caudate	384	–12	24	2	4.63	<.001
Right Parahippocampal gyrus (BA35–36)	134	30	–20	–28	3.64	<.001

Note. Abbreviations: BA = Brodmann area; ICDs = impulse control disorder.

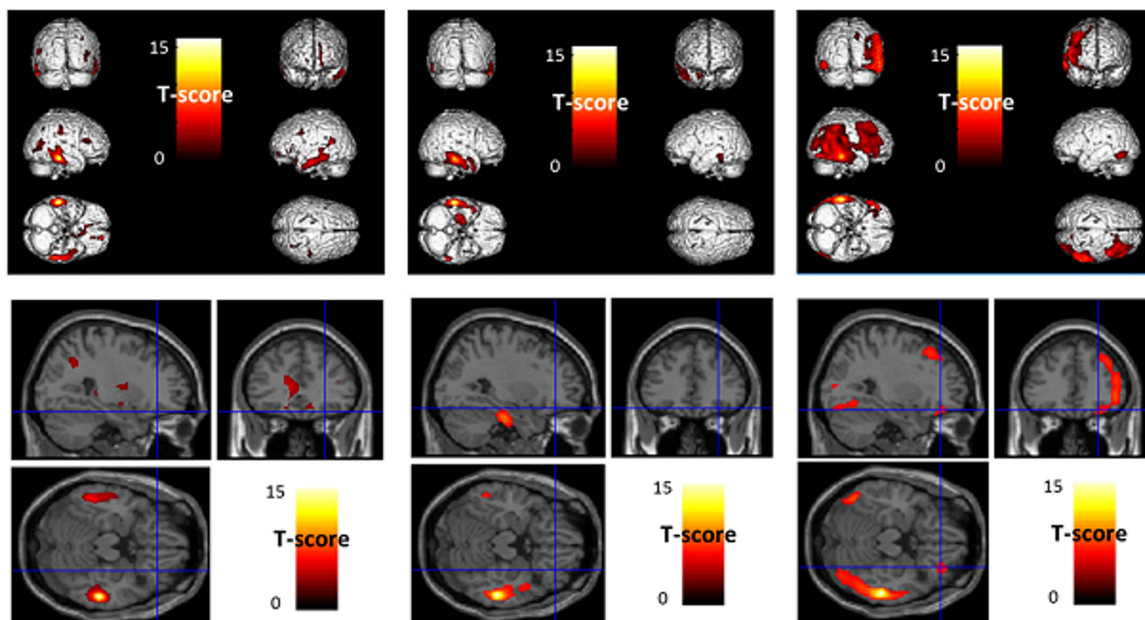


FIGURE 2 Anatomical localization of areas of increased positive right BA20–21 connectivity in healthy controls (left panel), in patients without ICDs (middle panel) and in patients with ICDs (right panel), projected onto 3D volume rendering (upper panel) and sections of a normal MRI (lower panel) set spatially normalized and smoothed into the standard SPM8 template ($p < .005$, uncorrected, $k > 130$). Healthy controls and patients without ICDs showed a moderately quite similar connectivity pattern involving bilateral temporal lobes (left and middle upper panel). Additional connectivity was only found in healthy subjects for fronto-parietal regions (left upper panel), without extension to orbito-frontal area (left lower panel). On the other hand, patients with ICDs showed a diffuse connectivity in bilateral posterior temporal lobes and right fronto-parietal lobes (right upper panel) including the orbito-frontal area (right lower panel). BA: Brodmann area; ICD: impulse control disorder; MRI: magnetic resonance imaging [Color figure can be viewed at wileyonlinelibrary.com]

temporal lobes and right fronto-parietal lobes including the orbito-frontal area. On the other hand, patients without ICDs and healthy controls showed a similar more moderate positive connectivity pattern involving bilateral temporal lobes. Additional connectivity was found in healthy subjects for fronto-parietal regions (Figure 2). No extension to the orbito-frontal area was found for healthy subjects or for PD patients without ICDs, and thus only for PD patients with ICDs.

Direct comparison of the right middle/inferior temporal gyri connectivity was thereafter performed between PD patients with and without ICDs. It first showed an increase of positive connectivity in ICD patients involving the right middle temporal gyrus (BA20–21–22), right middle and superior temporal gyri, right parietal inferior lobule (BA37–39–40), and right middle and inferior frontal gyri (BA9–10) including the right orbito-frontal area (BA11) (Figure 3). An increase of negative connectivity was also found in patients with ICDs, in comparison to those without ICDs, involving the left caudate and the right parahippocampal gyrus (BA35–36) ($p < .005$, uncorrected, $k > 130$; Figure 3). Detailed coordinates of all these findings are available in Table 2.

In light of the above, and knowing that the mesocorticolimbic system is suspected to be involved in the pathophysiology of ICDs (Cilia et al., 2008), we studied potential interactions between the right middle/inferior temporal cluster and the mesocorticolimbic system (a correlations graph summarizing correlation coefficients between right middle and inferior temporal gyri and mesocorticolimbic system is available in Figure 4). A subgraph containing the mesocorticolimbic system (bilateral amygdala, caudate, putamen, hippocampus, and fronto-orbital

cortex and midbrain) and the above-cited cluster was created in BRAPH, and a comparison of nodal measures between patients with and without ICDs and healthy subjects was performed.

In comparison with patients without ICDs, those with ICDs had a lower betweenness centrality in the left superior fronto-orbital cortex and in the right middle/inferior temporal cluster ($p = .04$) (Figure 5), meaning that the central place occupied by left superior fronto-orbital cortex and the above-cited cluster with the mesocorticolimbic system's connectivity is lost in patients with ICDs. Interestingly, patients with ICDs had also a lower betweenness centrality in comparison with healthy subjects, but only in the above-cited cluster ($p < .01$). There was no significant difference between patients without ICDs and healthy subjects, in particular for the betweenness centrality ($p = .22$). No other parameters compared between patients with and without ICDs (degree, strength, triangles, eccentricity, path length, global and local efficiency, clustering nodes, closeness centrality, and within module z-score degree) were significantly different for the above-cited cluster.

4 | DISCUSSION

This study shows that PD patients with ICDs had a relative increased PET metabolism within the right middle and inferior temporal regions (BA20–21), in comparison to PD patients without ICDs. Metabolism of this area was even higher in patients with multiple ICDs than in patients with a single ICD. These metabolic changes were interestingly associated with concomitant changes in metabolic connectivity of this

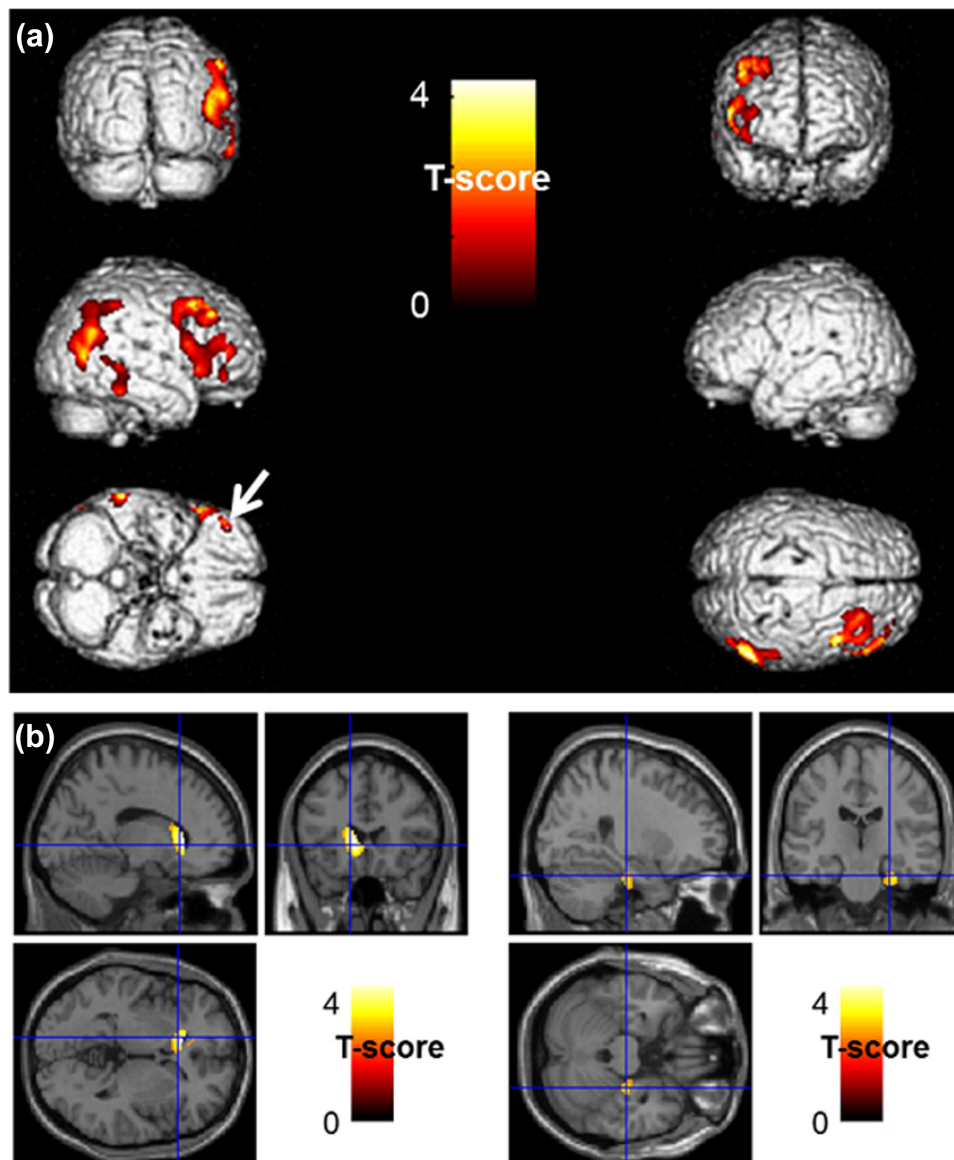


FIGURE 3 Anatomical localization of areas of increased positive (upper panel in a) and negative (lower panel in b) right BA20–21 connectivity in ICD patients in comparison to those without ICDs ($p < .005$, uncorrected, $k > 130$) projected onto 3D volume rendering (a) and sections of a normal MRI (b) set spatially normalized and smoothed into the standard SPM8 template. ICD patients showed an increased positive connectivity in right middle temporal gyrus (BA20–21–22), right middle and superior temporal gyri and parietal inferior lobule (BA37–39–40) and right middle and inferior frontal gyri (BA9–10), including the orbito-frontal area (BA11) (white arrow) (a). Moreover, ICD patients showed an increase negative connectivity with the left caudate (left panel), and with the right parahippocampal gyrus (BA35–36, right panel) (b). BA: Brodmann area; ICD: impulse control disorder; MRI: magnetic resonance imaging [Color figure can be viewed at wileyonlinelibrary.com]

same area. In ICD patients, BA20–21 had an increase of negative connectivity with the striato-limbic network; and on the opposite, a wide positive connectivity increase with right fronto-parietal gyri including the right orbito-frontal area. Moreover, BA20–21 area loses its central place with the mesocorticolimbic system through a connectivity dysregulation.

In ICD patients with PD, we here found an involvement of the right middle and inferior temporal gyri. This area is known to be involved in memory process, especially for visual modality (Smolka et al., 2006), and for both encoding and retrieval (Vaidya, Zhao, Desmond, & Gabrieli, 2002). In this line, Cilia et al. (2011) have found

positive correlations between gambling score and perfusion in temporal lobe, precisely the fusiform gyrus; and several studies in patients with substance use disorders have shown an activation of these temporal areas when visualizing drug-related cues (Park et al., 2007; Smolka et al., 2006; Wexler et al., 2001). In addition, increased perfusion of medial temporal region was found in a PD patient with dopamine agonist-related hypersexuality (Kataoka, Shinkai, Inoue, & Satoshi, 2009). Finally, these regions are known to be closely connected to the mesocorticolimbic system (Cooper, 2002), whose the involvement has been reported at rest (Koehler et al., 2013) and even during task (van Holst, Veltman, Büchel, van den Brink, & Goudriaan, 2012) in

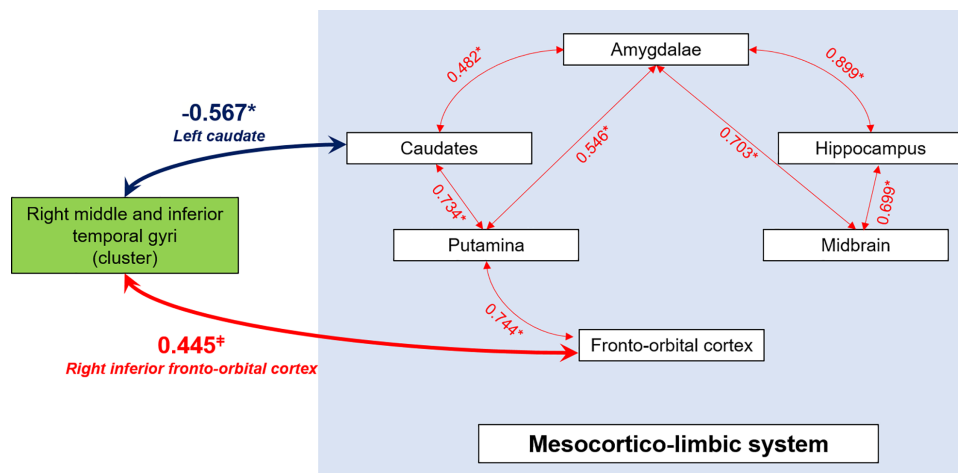


FIGURE 4 Correlations graph in patients with ICD between right middle and inferior temporal gyri (BA20–21) and the mesocorticolimbic system. Spearman correlation coefficients are indicated on the Figure. In patients with ICD, right middle and inferior temporal gyri (BA20–21) exhibit decreased connectivity with the left caudate, and a trend for increased connectivity with the right inferior fronto-orbital cortex. * $p < .05$, $\ddagger p = .06$ [Color figure can be viewed at wileyonlinelibrary.com]

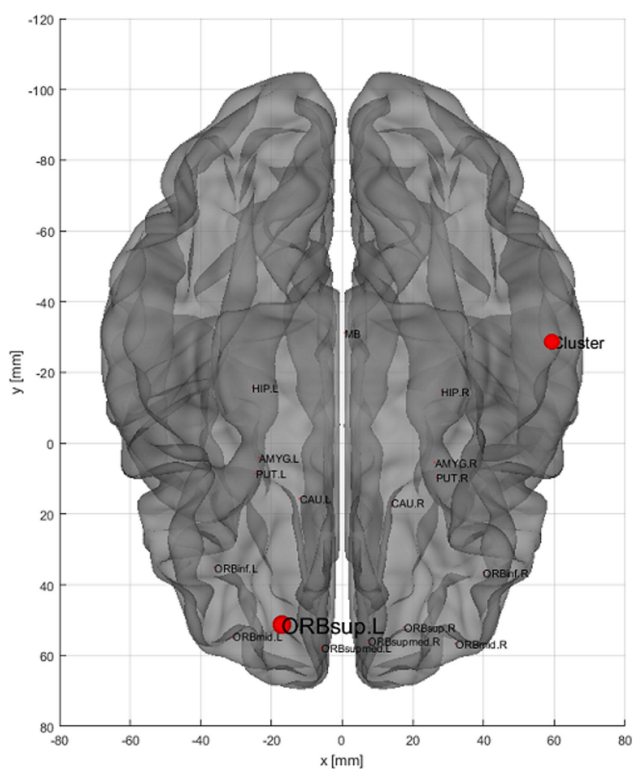


FIGURE 5 Three-dimensional volume rendering of the comparison of nodal measure betweenness centrality between patients with and without ICDs within the subgraph including BA20–21 and the mesocorticolimbic system (bilateral amygdala, caudate, putamen, hippocampus, and fronto-orbital cortex and midbrain), obtained after graph theory analysis. Between BA20–21 and the mesocorticolimbic system, the betweenness centrality is only decreased in the left superior orbito-frontal cortex (ORBsup.L) and the cluster (red points) in the patients with ICDs comparatively to the patients without ICDs ($p < .05$) [Color figure can be viewed at wileyonlinelibrary.com]

pathological gambling without PD. The main areas involved were specifically the striatum and the prefrontal cortex, particularly the orbito-frontal cortex.

Moreover, in comparison to PD patients without ICDs, patients with ICDs showed an increase of negative connectivity of the right BA20–21 with the left caudate and with the right parahippocampal region. These findings are in accordance with previous studies showing functional disconnection involving the mesocorticolimbic system in patients with ICDs and PD (Carriere et al., 2015; Cilia et al., 2011). In details, Cilia and al. showed anterior cingulate cortex-striatal disconnection in a SPECT study (Cilia et al., 2011); and Carriere et al. (2015) found fMRI disconnection exceeding the mesocorticolimbic system, between associative striatum (i.e., dorsal caudate and anterior putamen) and associative cortical regions including the inferior temporal region. We hypothesize this temporo-limbic disconnection disrupts the integration of information about the reward, contributing to the formation of the addictive process.

However, in contrast to other functional imaging studies (Carriere et al., 2015; Cilia et al., 2011), we report an increased connectivity in PD with ICDs. This involved the connectivity of the right BA20–21 areas with remotely: the right associative posterior junction and dorso-lateral frontal cortex extended to the orbitofrontal region. These connectivity increases were specific to patients with ICDs as illustrated by Figure 2. These areas are part of the Salience Network (Seeley et al., 2007), which is involved in the detection and orientation to the most pertinent external or internal stimuli presented (Menon, 2011). Interestingly, our results are in accordance with another fMRI study (Tessitore et al., 2017) where the connectivity of this Salience Network was also increased in PD patients with ICDs. In addition, in PD, Cilia et al. (2008) reported also an increased SPECT perfusion of orbito-frontal region in patients with ICDs. Tahmasian et al. (2015) suggest that the hyperactivity of the orbitofrontal cortex is essential for adapted inhibition of behaviors in PD patients with high impulsivity. Nevertheless, it remains impossible to formally determining whether

the frontal regions have a role in inhibiting behavior among ICD patients or rather causally involved in the genesis of ICDs.

Concerning the community composed by the mesocorticolimbic system and the cluster and their relationships, betweenness centralities of the left superior fronto-orbital cortex and the cluster were lower in patients with ICDs than in patients without ICDs as illustrated in Figure 5, but also than in healthy subjects in the case of the cluster. That means that patients with ICDs lose the central place of BA20–21 area with mesocorticolimbic system's connectivity (Mijalkov et al., 2017). Changes of connectivity within the temporal lobe have already been described in PD patients (Chen et al., 2017; Shah et al., 2017; Zhang et al., 2017). Considering that there is no significant difference between patients without ICDs and healthy subjects for the betweenness centrality ($p = .22$) and that no other parameters compared between patients with and without ICDs were significantly different for the left superior fronto-orbital cortex and the above-cited cluster, those two cerebral areas in patients with ICDs seem to have lost their central function with the mesocorticolimbic system, through a connectivity dysregulation. Thus, the increased metabolism of BA20–21 area in patients with ICDs could be a way to compensate for this lack of effectiveness. Furthermore, increased connectivity mainly in mesocorticolimbic system, observed with BA20–21 in ICD patients in a positive or negative way, seems to correspond to a dysregulation phenomenon. Overall, this cluster seems involved either as a cause or a consequence in the physiopathology of ICDs.

This study has some limitations. First, our specific population involved various ICDs whereas previous studies focused only on pathologic gamblers (Carriere et al., 2015; Cilia et al., 2011). In addition, 3 of our ICD patients had criteria of dopamine dysregulation syndrome. These results could thus reflect a common mechanism for ICDs rather than being specific to only one type. Furthermore, our patients with ICDs and without ICDs presented at least a 5 years of disease duration which may have interfered with metabolic findings, a long PD duration being associated with diffuse metabolic impairments (Eidelberg, 2009). However, there was no significant difference in the duration of disease between patients with ICD and those without ICD, going against a different cognitive level between the two groups. In this line, no difference was observed in Mattis score between PD patients and healthy subjects. Otherwise, we decided to study brain metabolism as a whole at voxel-level, contrary to most previous functional connectivity studies based on analysis of selected regions of interest (Carriere et al., 2015; Tessitore et al., 2017). This overall approach leads to a potential increase of confounding factors in the results for these patients with a neurodegenerative disease and with potential entangled pathophysiological phenomenon exceeding ICDs networks. Nevertheless, this risk was limited by the selection of two groups, with and without ICDs, very similar on other clinical data. In addition, it provides a more general approach of brain networks involved, exceeding herein the commonly described mesocortico- limbic system.

5 | CONCLUSION

On the whole, this study shows that ICDs in PD are associated with the dysfunction of a large network exceeding the mesocorticolimbic

system, and involving especially the caudate, the parahippocampus, and the prefrontal cortex, remotely including the right middle and inferior temporal gyri. This latest area loses its central place with the mesocorticolimbic system corresponding to a connectivity dysregulation. We hypothesize that these regions are particularly involved in the establishment of a mnemonic component of addiction. This hypothesis will require further experimental paradigms to be confirmed. Whether these regions are involved either as a cause or a consequence in the physiopathology of ICDs also remains to be established.

ACKNOWLEDGMENTS

This work has been carried out thanks to the support of the A*MIDEX project (n° ANR-11-IDEX-0001-02) funded by the "Investissements d'Avenir" French Government program, managed by the French National Research Agency (ANR). This work was also supported by Inserm (Centre d'Investigation Clinique, CIC, Hôpital de la Conception, Marseille), and AP-HM (PHRC 2007/09).

ORCID

Eric Guedj  <http://orcid.org/0000-0003-1912-6132>

REFERENCES

- Bailey, D. L., & Willows, K. P. (2014). Quantitative SPECT/CT: SPECT joins PET as a quantitative imaging modality. *European Journal of Nuclear Medicine and Molecular Imaging*, 41(Suppl 1), S17–S25.
- Carriere, N., Lopes, R., Defebvre, L., Delmaire, C., & Dujardin, K. (2015). Impaired corticostriatal connectivity in impulse control disorders in Parkinson disease. *Neurology*, 84(21), 2116–2123.
- Chen, B., Wang, S., Sun, W., Shang, X., Liu, H., Liu, G., ... Fan, G. (2017). Functional and structural changes in gray matter of parkinson's disease patients with mild cognitive impairment. *European Journal of Radiology*, 93, 16–23.
- Cilia, R., Cho, S. S., van Eimeren, T., Marotta, G., Siri, C., Ko, J. H., ... Strafella, A. P. (2011). Pathological gambling in patients with Parkinson's disease is associated with fronto-striatal disconnection: A path modeling analysis. *Movement Disorders*, 26(2), 225–233.
- Cilia, R., Siri, C., Marotta, G., Isaias, I. U., De Gaspari, D., Canesi, M., ... Antonini, A. (2008). Functional abnormalities underlying pathological gambling in Parkinson disease. *Archives of Neurology*, 65(12).
- Cooper, D. C. (2002). The significance of action potential bursting in the brain reward circuit. *Neurochemistry International*, 41(5), 333–340.
- D'Ardenne, K., McClure, S. M., Nystrom, L. E., & Cohen, J. D. (2008). BOLD responses reflecting dopaminergic signals in the human ventral tegmental area. *Science*, 319, 1264–1267.
- Defer, G.-L., Widner, H., Marié, R.-M., Rémy, P., & Levivier, M. (1999). Core assessment program for surgical interventional therapies in Parkinson's disease (CAPSIT-PD). *Movement Disorders*, 14(4), 572–584.
- Eidelberg, D. (2009). Metabolic brain networks in neurodegenerative disorders: A functional imaging approach. *Trends in Neurosciences*, 32(10), 548–557.
- Fox, M. D., & Greicius, M. (2010). Clinical applications of resting state functional connectivity. *Frontiers in Systems Neuroscience*, 4, 19.
- Frosini, D., Pesaresi, I., Cosottini, M., Belmonte, G., Rossi, C., Dell'Osso, L., ... Ceravolo, R. (2010). Parkinson's disease and pathological gambling: Results from a functional MRI study. *Movement Disorders*, 25(14), 2449–2453.

- Gesquière-Dando, A., Guedj, E., Loundou, A., Carron, R., Witjas, T., Fluchère, F., ... Eusebio, A. (2015). A preoperative metabolic marker of parkinsonian apathy following subthalamic nucleus stimulation. *Movement Disorders*, 30(13), 1767–1776.
- Giovannoni, G., O'Sullivan, J. D., Turner, K., Manson, A. J., & Lees, A. J. (2000). Hedonistic homeostatic dysregulation in patients with Parkinson's disease on dopamine replacement therapies. *Journal of Neurology, Neurosurgery, and Psychiatry*, 68(4), 423–428.
- van Holst, R. J., Veltman, D. J., Büchel, C., van den Brink, W., & Goudriaan, A. E. (2012). Distorted expectancy coding in problem gambling: Is the addictive in the anticipation? *Biological Psychiatry*, 71(8), 741–748.
- Holtgraves, T., McNamara, P., Cappaert, K., & Durso, R. (2010). Linguistic correlates of asymmetric motor symptom severity in Parkinson's Disease. *Brain and Cognition*, 72(2), 189–196.
- Kaiser, R. H., Andrews-Hanna, J. R., Wager, T. D., & Pizzagalli, D. A. (2015). Large-scale network dysfunction in major depressive disorder: A meta-analysis of resting-state functional connectivity. *JAMA Psychiatry*, 72(6), 603.
- Kataoka, H., Shinkai, T., Inoue, M., & Satoshi, U. (2009). Increased medial temporal blood flow in Parkinson's disease with pathological hypersexuality. *Movement Disorders*, 24(3), 471–473.
- Koehler, S., Ovidia-Caro, S., van der Meer, E., Villringer, A., Heinz, A., Romanczuk-Seiferth, N., & Margulies, D. S. (2013). Increased functional connectivity between prefrontal cortex and reward system in pathological gambling. *PLoS One*, 8(12), e84565.
- Koob, G. F., & Volkow, N. D. (2010). Neurocircuitry of addiction. *Neuropharmacology*, 35(1), 217–238.
- Lee, D. S., Kang, H., Kim, H., Park, H., Oh, J. S., Lee, J. S., & Lee, M. C. (2008). Metabolic connectivity by interregional correlation analysis using statistical parametric mapping (SPM) and FDG brain PET; methodological development and patterns of metabolic connectivity in adults. *European Journal of Nuclear Medicine and Molecular Imaging*, 35(9), 1681–1691.
- Lieberman, M. D., & Cunningham, W. A. (2009). Type I and Type II error concerns in fMRI research: Re-balancing the scale. *Social Cognitive and Affective Neuroscience*, 4(4), 423–428.
- Llebaria, G., Pagonabarraga, J., Kulisevsky, J., García-Sánchez, C., Pascual-Sedano, B., Gironell, A., & Martínez-Corral, M. (2008). Cut-off score of the Mattis Dementia Rating Scale for screening dementia in Parkinson's disease. *Movement Disorders*, 23(11), 1546–1550.
- Magistretti, P. J., & Pellerin, L. (1999). Cellular mechanisms of brain energy metabolism and their relevance to functional brain imaging. *Philosophical Transactions of the Royal Society of London. Series B, Biological Sciences*, 354(1387), 1155–1163.
- Maréchal, E., Denoix, B., Thys, E., Crosiers, D., Pickut, B., & Cras, P. (2015). Impulse control disorders in Parkinson's disease: An overview from neurobiology to treatment. *Journal of Neurology*, 262(1), 7–20.
- Menon, V. (2011). Large-scale brain networks and psychopathology: A unifying triple network model. *Trends in Cognitive Sciences*, 15(10), 483–506.
- Mijalkov, M., Kakaie, E., Pereira, J. B., Westman, E., & Volpe, G. for the Alzheimer's Disease Neuroimaging Initiative (2017). BRAPH: A graph theory software for the analysis of brain connectivity. Ed. *PLoS One*, 12(8), e0178798.
- Nombela, C., Rittman, T., Robbins, T. W., & Rowe, J. B. (2014). Multiple modes of impulsivity in Parkinson's disease. *PLoS One*, 9(1), e85747.
- Park, M.-S., Sohn, J.-H., Suk, J.-A., Kim, S.-H., Sohn, S., & Sparacio, R. (2007). Brain substrates of craving to alcohol cues in subjects with alcohol use disorder. *Alcohol and Alcoholism (Oxford, Oxfordshire)*, 42(5), 417–422.
- Pereira, J. B., Aarsland, D., Ginestet, C. E., Lebedev, A. V., Wahlund, L.-O., Simmons, A., ... Westman, E. (2015). Aberrant cerebral network topology and mild cognitive impairment in early Parkinson's disease: Aberrant Brain Network Topology in Early PD. *Human Brain Mapping*, 36(8), 2980–2995.
- Seeley, W. W., Menon, V., Schatzberg, A. F., Keller, J., Glover, G. H., Kenna, H., ... Greicius, M. D. (2007). Dissociable intrinsic connectivity networks for salience processing and executive control. *Journal of Neuroscience*, 27(9), 2349–2356.
- Shah, A., Lenka, A., Saini, J., Wagle, S., Naduthota, R. M., Yadav, R., ... Ingalhalikar, M. (2017). Altered brain wiring in Parkinson's disease: A structural connectome-based analysis. *Brain Connectivity*, 7(6), 347–356.
- Smolka, M. N., Bühler, M., Klein, S., Zimmermann, U., Mann, K., Heinz, A., & Braus, D. F. (2006). Severity of nicotine dependence modulates cue-induced brain activity in regions involved in motor preparation and imagery. *Psychopharmacology*, 184(3–4), 577–588.
- Tahmasian, M., Rochhausen, L., Maier, F., Williamson, K. L., Drzezga, A., Timmermann, L., ... Eggers, C. (2015). Impulsivity is associated with increased metabolism in the fronto-insular network in Parkinson's disease. *Frontiers in Behavioral Neuroscience*, 9.
- Tessitore, A., Santangelo, G., De Micco, R., Giordano, A., Raimo, S., Amboni, M., ... Vitale, C. (2017). Resting-state brain networks in patients with Parkinson's disease and impulse control disorders. *Cortex*, 94, 63–72.
- Tomlinson, C. L., Stowe, R., Patel, S., Rick, C., Gray, R., & Clarke, C. E. (2010). Systematic review of levodopa dose equivalency reporting in Parkinson's disease. *Movement Disorders*, 25(15), 2649–2653.
- Vaidya, C. J., Zhao, M., Desmond, J. E., & Gabrieli, J. D. E. (2002). Evidence for cortical encoding specificity in episodic memory: Memory-induced re-activation of picture processing areas. *Neuropsychologia*, 40(12), 2136–2143.
- Weintraub, D., Koester, J., Potenza, M. N., Siderowf, A. D., Stacy, M., Voon, V., ... Lang, A. E. (2010). Impulse control disorders in Parkinson disease: A cross-sectional study of 3090 patients. *Archives of Neurology*, 67(5), 589–595.
- Wexler, B. E., Gottschalk, C. H., Fulbright, R. K., Prohovnik, I., Lacadie, C. M., Rounsaville, B. J., & Gore, J. C. (2001). Functional magnetic resonance imaging of cocaine craving. *American Journal of Psychiatry*, 158(1), 86–95.
- Witjas, T., Eusebio, A., Fluchère, F., & Azulay, J.-P. (2012). Addictive behaviors and Parkinson's disease. *Revue Neurologique*, 168(8–9), 624–633.
- Yakushev, I., Drzezga, A., & Habeck, C. (2017). Metabolic connectivity: Methods and applications. *Current Opinion in Neurology*, 30(6), 677–685.
- Zhang, J.-J., Ding, J., Li, J.-Y., Wang, M., Yuan, Y.-S., Zhang, L., ... Zhang, K.-Z. (2017). Abnormal resting-state neural activity and connectivity of fatigue in Parkinson's disease. *CNS Neuroscience & Therapeutics*, 23(3), 241–247.
- Zhang, S., Dissanayaka, N. N., Dawson, A., O'sullivan, J. D., Mosley, P., Hall, W., & Carter, A. (2016). Management of impulse control disorders in Parkinson's disease. *International Psychogeriatrics*, 1–18.

How to cite this article: Verger A, Klesse E, Chawki MB, et al. Brain PET substrate of impulse control disorders in Parkinson's disease: A metabolic connectivity study. *Hum Brain Mapp*. 2018;39:3178–3186. <https://doi.org/10.1002/hbm.24068>